RESEARCH ARTICLE | APRIL 24 2023

Imposing residual stress within micro fin model to understand the deformation caused by WEDM

Warregh Adel ✉; Z. M. Zahiruddin

AIP Conf. Proc. 2544, 040023 (2023)
https://doi.org/10.1063/5.0118192

Imposing Residual Stress within Micro Fin Model to Understand the Deformation Caused by WEDM

Warregh Adel[a)] and Z M Zahiruddin

Faculty of Mechanical Engineering Technology, Universiti Malaysia Perlis, Kampus Tetap Pauh Putra, 02600 Arau, Perlis, Malaysia.

[a)]Corresponding author: adelsaleh201313@yahoo.com

Abstract. This work describes a method of applying residual stress within micro fin model to understand the deformation of the fin machined by wire electrical discharge machining (WEDM). Firstly, transient temperature distribution on a workpiece caused by WEDM discharges was calculated using finite element method (FEM). Then, the result was used to calculate the residual stress. It was found that the residual stress in the radial direction, $\sigma_r(z)$ along the centre axis of each discharge crater was distributed non-linearly in thickness direction from the crater top surface. Then, based on structural analysis, the $\sigma_r(z)$ was imposed within the micro fin model. Here, thermal stress field caused by series of sequential discharges was considered. The summation of calculated deflections after three sequential discharges was approximately equal to the measurement result. As a result, the non-linear distribution of $\sigma_r(z)$ was found to be the main reason that causes the non-uniform bending of the micro fin.

INTRODUCTION

Electrical discharge machining (EDM) can make micro components with intricate features out of any electrically conductive material, regardless of hardness. However, at certain sizes and geometries, deformation of the EDM workpiece affects the dimensional stability and accuracy of the part, limiting further miniaturization of the process. The deformation could be caused by two types of residual stress. The first is residual stress in the workpiece prior to machining [1], and the second is residual stress induced by EDM [2]. The stress that exists prior to machining is the result of plastic deformation processes such as forging and wire drawing. The annealing process can be used to release this kind of residual stress before the machining process [1]. During EDM, On the other hand, only part of the region on the workpiece where the temperature is above melting point is removed and the remaining molten region is left in the crater to form a recast layer. While the region near crater is in a molten state, no residual stress will be formed due to free movement. However, the recast layer solidifies at the end of discharge, and the cooling process begins. The tensile residual stress is formed at the cooling region, causing the region near the crater to contract [2] [3] [4].

Even after the workpiece had been annealed, fabricated fins began to fold in WEDM when the fin thickness was less than 100 m in rough cutting condition, indicating that the phenomenon was due to the EDM [2]. Thermal deformation cannot be overlooked because it has the potential to affect component output during use [5 - 7], especially for thin-walled components. The residual stress caused by the WEDM operation, on the other hand, has yet to be fully clarified. Furthermore, no other studies have looked into the effect of residual stress on workpiece deformation. As a result, thermal and structural analyses are carried out in this work in order to understand the deformation. Residual stress due to discharges is calculated from the heat conduction model within the workpiece. Then, the obtained residual stress is imposed within the micro fin model in structural analysis to understand the deformation of the micro fin. This work aims to: (1) develop an efficient 2D finite element model to simulate the temperature gradients; (2) imposing residual stress within micro fin model in order to understand the behaviour of micro fin deformation induced from a single pulse discharge.

Proceeding of the 1st International Conference on Manufacturing Engineering Technology (IConMET 2021)
AIP Conf. Proc. 2544, 040023-1–040023-14; https://doi.org/10.1063/5.0118192
Published by AIP Publishing. 978-0-7354-4322-8/$30.00

EXPERIMENTAL SETUP

Preparation of Workpiece Material

The stainless steel grade AISI 316 was chosen as the workpiece material, with dimensions of 200 mm x 100 mm x 3 mm (see Fig. 1).As demonstrated in Fig. 2, the workpiece was cut using WEDM to produce a micro fin. The tool electrode in this study was a brass wire with a diameter of 0.25 mm.

FIGURE 1. AISI 316 workpiece.

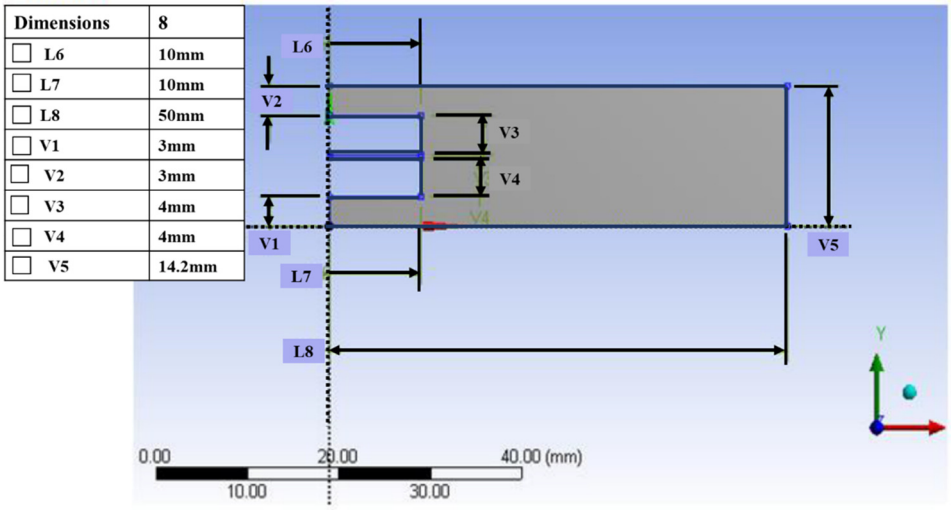

FIGURE 2. Dimensions of fabricated micro fin.

Machine Setup

In this study, a Sodick AQ327L WEDM machine was used with deionized water as the dielectric (see Fig. 3). Setup of AQ327L and the machining area is demonstrated in Fig. 4.

FIGURE 3. Wire cut machine

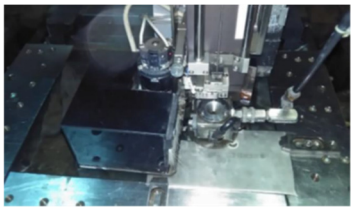

FIGURE 4. Setup of AQ327L

Properties of Workpiece Material

The thermal and mechanical properties of stainless steel grade AISI 316 is seen in Table 1.

TABLE 1. Thermal and mechanical properties of AISI 316

Thermal properties	Unit	Value
Thermal conductivity	W/m K	16.3
Coefficient of thermal expansion	K^{-1}	15.9×10^{-6}
Specific heat	J/kg K	500
Density	Kg/m^3	8000
Melting temperature	K	1673
Mechanical properties		
Modulus of elasticity	G Pa	200
Poisson's ratio	---	0.275
Tensile yield strength	M Pa	579

Machining Settings for the Experiment

The machining parameters settings used in this study are as follows:
The open circuit voltage is 120 V, and the peak current is 10 A. The pulse on time is 100 µs. Other machining parameters such as polarity, dielectric fluid, wire tension, wire control, water pressure, servo speed, frequency constant, and wire speed, which are mentioned in Table 2, were held constant.

TABLE 2. Other machining settings of WEDM

Parameters	Unit	Values
Shape and size of workpiece	---	Rectangular, 50 × 14.5 × 3 mm
Angle of cut	---	Vertical
Dielectric temperature	K	298
Water pressure (0.1 Mpa)	MPa	24
Wire speed	m/s	0.29
Wire tension	N	15
Pulse off time	µ s	14
Wire feed rate	mm/min	0.5
Workpiece polarity	---	Positive (anode)
Electrode polarity	---	Negative (cathode)
Dielectric fluid	---	Deionized water
Type and diameter of wire	---	Brass, Ø250 µm
Servo speed	mm/min	0040
Wire control	---	025

SIMULATION METHODOLOGY

Assumptions of Modelling

The steel material melts at a comparatively high temperature during machining in current work, but the temperature rise is sufficient to melt the steel particles. Conduction is the mode of heat transfer in solids, and convection is the mode of heat transfer between the dielectric and the workpiece. It is important to consider temperature dependant structure

properties of the workpiece material. As a result, in this study, the elastic-perfectly plastic model was considered. The structure properties that were used in the calculation are seen in Fig. 5. Furthermore, based on the removal mechanism analysis, 11% of the molten region was removed during discharging. Consequently, removal of material is also considered when calculating residual stress due to WEDM single discharge. Besides that, there are other important assumptions that have been made regarding the model are follows:

i. The workpiece material is homogeneous and isotropic, also the workpiece domain is considered axisymmetric [13].
ii. The material's thermophysical properties are temperature-based.
iii. Prior to WEDM, the workpiece is stress-free [13].
iv. Except for the discharge region, all surfaces in the model are adiabatic.
v. The workpiece's initial temperature was set to room temperature (298 K), in addition, the heat source is assumed as a circular disk.
vi. The analysis is conducted only for a single discharge [13].

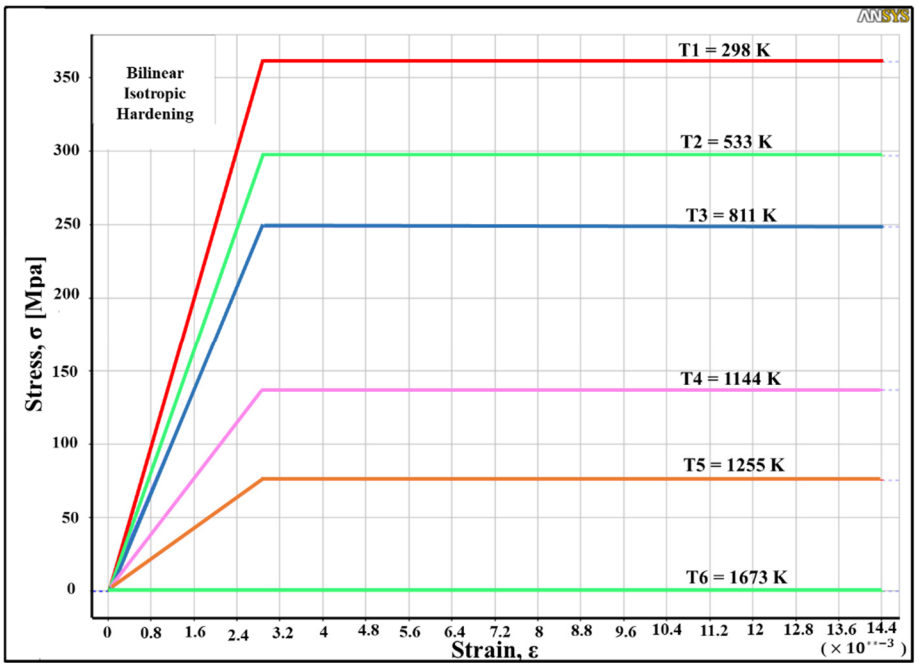

FIGURE 5. Temperature dependent bilinear hardening

Coupled-Field Analyses and Kinds of Element

In current work, thermal residual stress is calculated from the temperature profile of the workpiece model (based on the results of temperature distribution within the workpiece at the end of cooling time). This means, thermal and structural analyses are required in the calculation of the thermal residual stress. However, there are more than 150 different element types in Mechanical APDL (ANSYS 18.1). The selection of the type of element is very important to assure that the desired model can be developed and the desired output results can be obtained. In the present work, 2-dimensional 8 nodes coupled-field solid element (PLANE77) has been selected.

Simulation of Material Removal

Mechanical APDL (ANSYS 18.1) program has the capability of simulating material removal utilizing element killing feature. During the element killing, the ANSYS program does not actually remove the elements. It deactivates them by reducing their stiffness significantly in structural analysis. Fig. 6 demonstrates an example of material removal simulation using the element killing feature in ANSYS software.

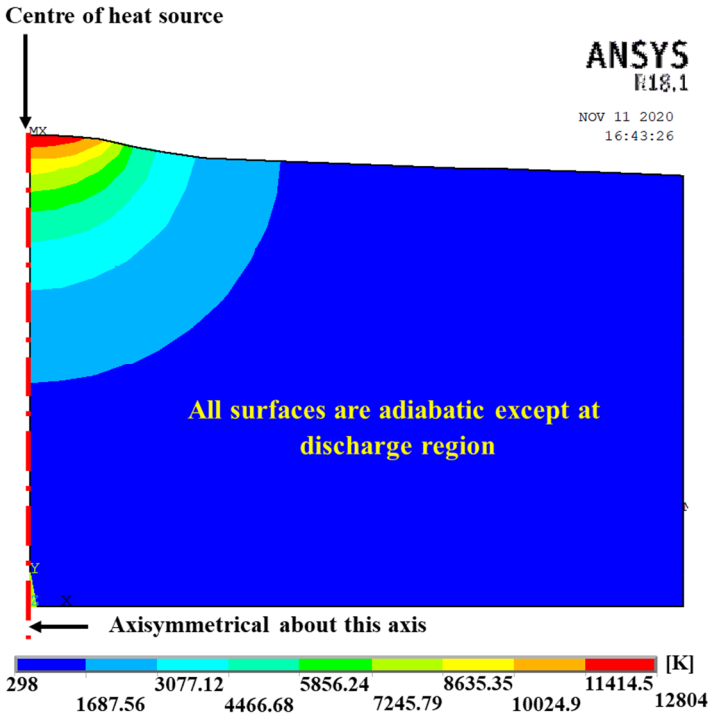

a. Before removal of deactivated elements

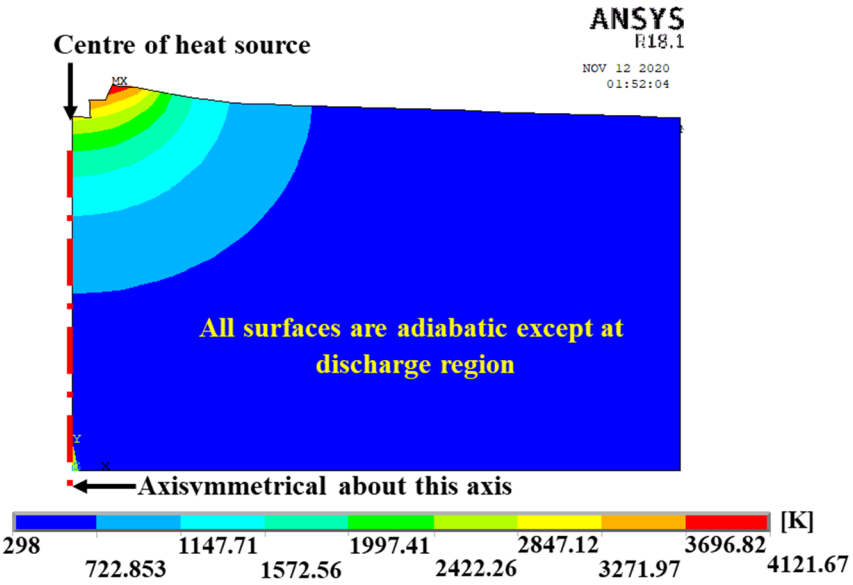

b. After removal of deactivated elements

FIGURE 6. Method to simulate material removal with respect to temperature rise

Theory of the Formation of Residual Stress and Micro fin Deformation

Tensile stress is formed and remains on both sides of the first slot after the first cutting, as seen in Fig. 7a. The stress of the part surface in the neighbouring area of the first slot is released during the second slot cutting. Tensile stress is formed in the area on the part surface adjacent to the second slot at the same time. When the part width, *pw* is small enough, tensile stress at the adjacent area of the second slot causes the part to bend toward this slot, as seen in Fig. 7

c. To obtain quantitatively the part curvature due to WEDM, it is necessary to conduct the structural analysis in order to calculate the workpiece deformation which was caused by the thermal stress [8].

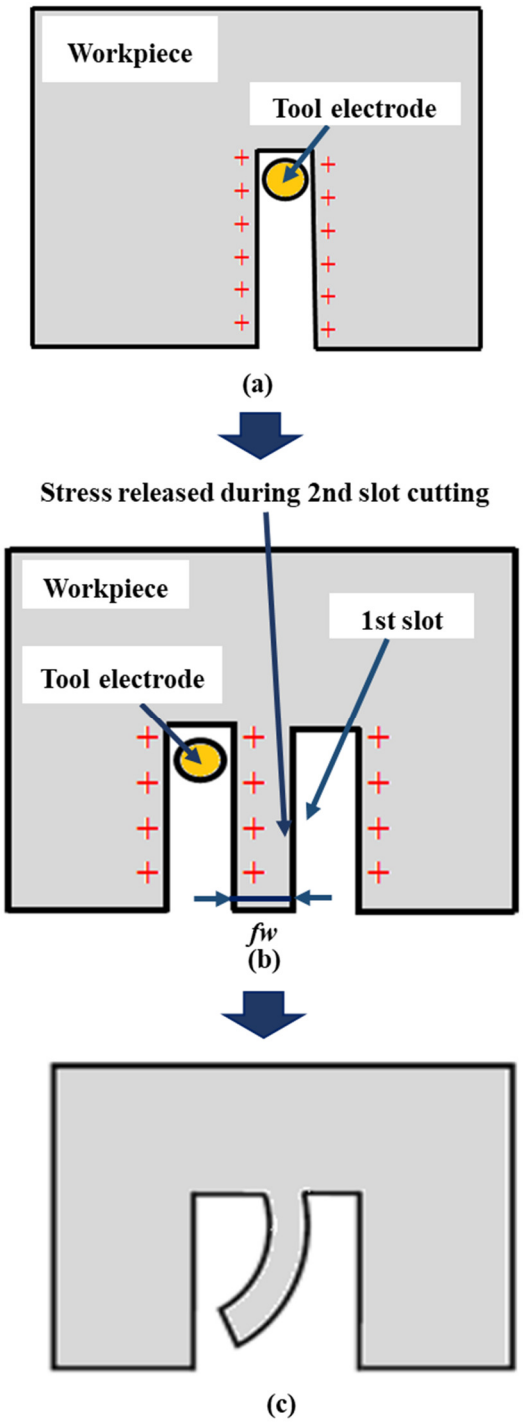

FIGURE 7. Theory of residual stress formation and micro fin deformation (a) Cutting first slot (b) Cutting second slot (c) Micro fin bends due to tensile stress

Approach to Impose Residual Stress

ANSYS provides several types of element that can be used for the structural analysis. Fig. 15 a. shows a picture of micro fin which was machined by WEDM in this study. As illustrated in the figure, the deformation of micro fin is not uniform along the axis. The fin looks curvature is larger near the tip and straight is near the root. One of the element types in ANSYS which are suitable to model curvature is PLANE 183. Therefore, PLANE 183 was selected as an element to build the micro fin model.

In addition, the element can be used for axisymmetric modelling and well suited for large deflection and large strain capability. Another capability of this element is allowing the application of 'initial state'. This is required in this study to impose the residual stress within the fin workpiece model. In order to impose the residual stress, ANSYS program uses INISTATE command. Thus, for each element, this command need to be typed manually within the ANSYS programme. The syntax is as follows:

'INISTATE, define, element #, , , , residual stress value'

For example, 'INISTATE, define, 675, , , , -2e+8' this mean that compressive residual stress of 2×10^8 Pa is imposed at element number 675. Here negative sign indicates compressive, and to impose tensile stress within an element no particular sign is required. In current work, a uniform rectangular beam model will be developed in order to clearly understand the effect of the residual stress which is non- linearly distributed in the thickness direction on the deformation of micro fin. The model size will be 0.2 mm ×10 mm and mesh size is made equal to 0.0067 mm. This means all together 44790 elements are involved, and thus 44790 syntaxes must be typed manually within the ANSYS program to define residual stress at each element.

Residual Stress due to Single Pulse Discharge

To build the heat conduction model, the power input of WEDM discharges is required. In WEDM, discharge energy per unit time distributed at workpiece under each unit area of circular surface heat source so-called power density, P_e was used as a measure of the power input. It is calculated as follows:

$$P_e = X \cdot i_e \cdot u_e / (\pi \cdot d^2/4) \quad (1)$$

Where:

• i_e and u_e are discharge current and discharge voltage, respectively which are measurable during discharging.

• X is the ratio of energy distributed into workpiece with respect to the total discharge energy, and it was found to be more than the case of micro EDM and lower than the case of sinking EDM [9].

• d is plasma diameter. In sinking EDM, plasma diameter expands about 5 times of crater diameter within the first 2 μs of t_e [10]. In this work t_e was 15 μs which is significantly longer than 2 μs. Thus, d in this work was calculated to be 96 μm [9].

Now all the parameters that are required to determine P_e in wire EDM are illustrated in **Table 3**, and in current work, they will be used for the thermal stress analysis. The physical model of heat conduction to estimate the residual stress was built using ANSYS software; finite element analysis software. Although the toughness of stainless steel is relatively high, it was found that the stainless steel workpiece are vulnerable to thermal deformation. The energy input as illustrated in **Table 3** was used to model the power density on the workpiece.

Fig. 8 illustrates an overview of the axisymmetric model, with 0.5 mm in radius and 0.3 mm in thickness. In this model, all surfaces were assumed adiabatic except the discharge area.

TABLE 3. WEDM power input

Parameter	Symbol	Unit	Value
Discharge current	i_e	A	4.5
Discharge voltage	u_e	V	20[12]
Discharge duration	t_e	μs	15
Energy distribution ratio into workpiece	X	%	32[12]
Plasma diameter	d	μm	96
Power density on workpiece	P_e	GW/m^2	4.0
Workpiece Material	---	---	AISI 316[12]
Dielectric medium	---	---	Water
Reference (ambient) temperature	---	K	298[12]

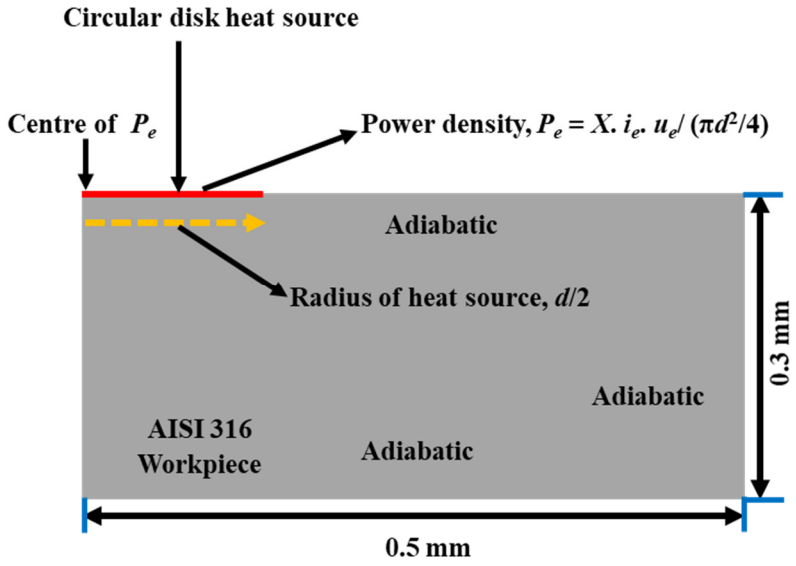

FIGURE 8. Heat conduction model of AISI 316 workpiece

Fig. 9 illustrates the magnification of the discharge area. The area in the workpiece where the temperature exceeds boiling point was assumed to vaporize immediately, and thus each element in the area was removed from the model. Accordingly, the power density location was changed as illustrated in Fig. 9.

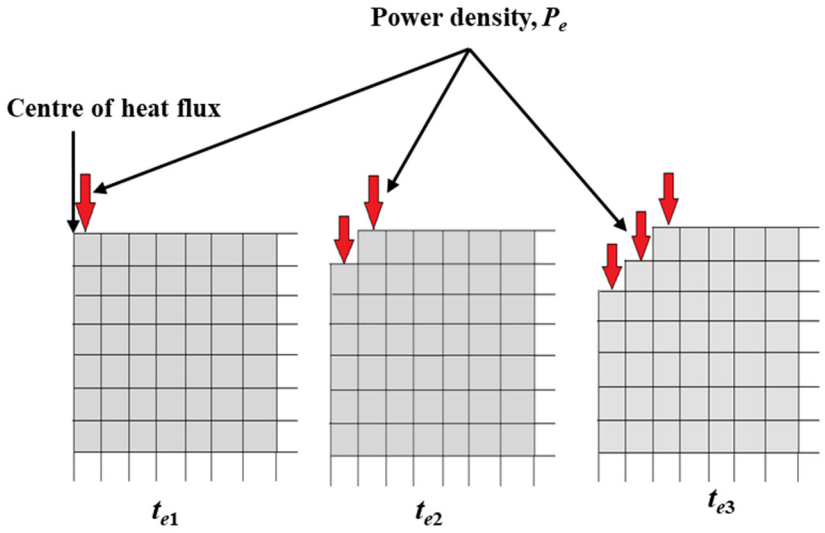

FIGURE 9. Magnifaction of discharge region with considering boundaries moving

In present work, the power density at AISI 316 workpiece, P_e can be calculated and it was found to be in the range between 400 to 4.0 GW/m^2. Where, the discharging time was divided into two intervals; the first interval is transient which starts from 0 to 2 μs, while the second interval is steady-state which starts from 2 to 15 μs. In the first interval, it was difficult to define plasma size and power density at 0 sec. Thus, during calculation, the initial value of plasma diameter and power density at electrode was made equal to the value at 0.2 μs of discharging time, where in this interval, the discharge duration was 2 μs, and divided into 10 time steps during calculation, which means 0.2 μs is the 2nd step of the total time steps. In the second interval, the plasma expanding was reach to maximum size (96 μm) at t_e = 2 μs, and remains at maximum diameter until end discharge duration at t_e =15 μs.

After the end of discharge, the simulation was continued to allow cooling before obtaining the residual stress. Fig. 10 illustrates the temperature distribution at the end of cooling (t = 95 μs after the ignition of discharge). As illustrated in the figure, the maximum temperature of the workpiece model drops to 365 K which is only 67 K above the initial temperature. This can be considered sufficiently low for the residual stress calculation.

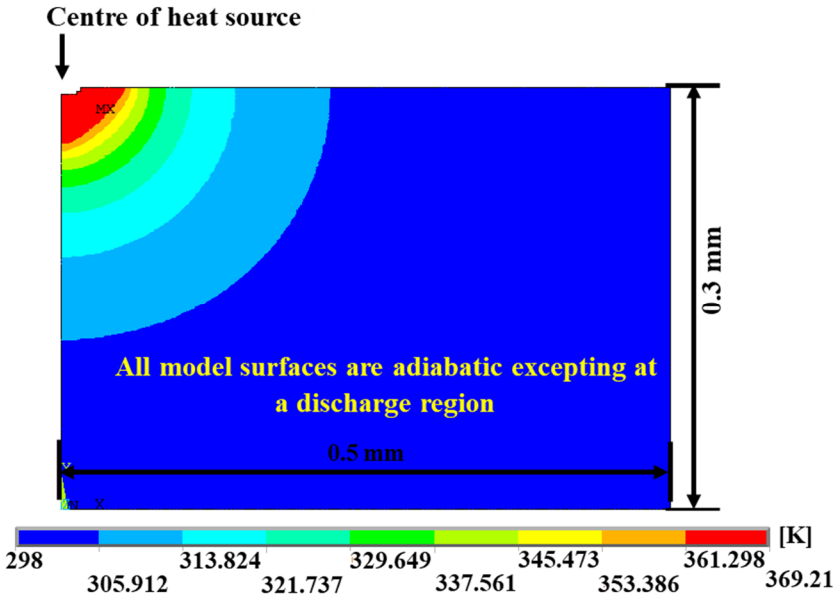

Figure 10. Temperature profile isotherms considering material removal at the end of cooling time

From this model (Fig. 10), the residual stress distribution along the center axis of a crater due to wire EDM single discharge was calculated. Fig. 11 illustrates the result of the residual stress in the radial direction, σ_r (z). As illustrated in the figure, the distribution of residual stress, σ_r (z) is non- linear, coinciding with the results obtained by other researchers [3] [4]. The effect of nonlinear distribution of residual stress, σ_r (z), on micro fin deformation will be observed in the later section.

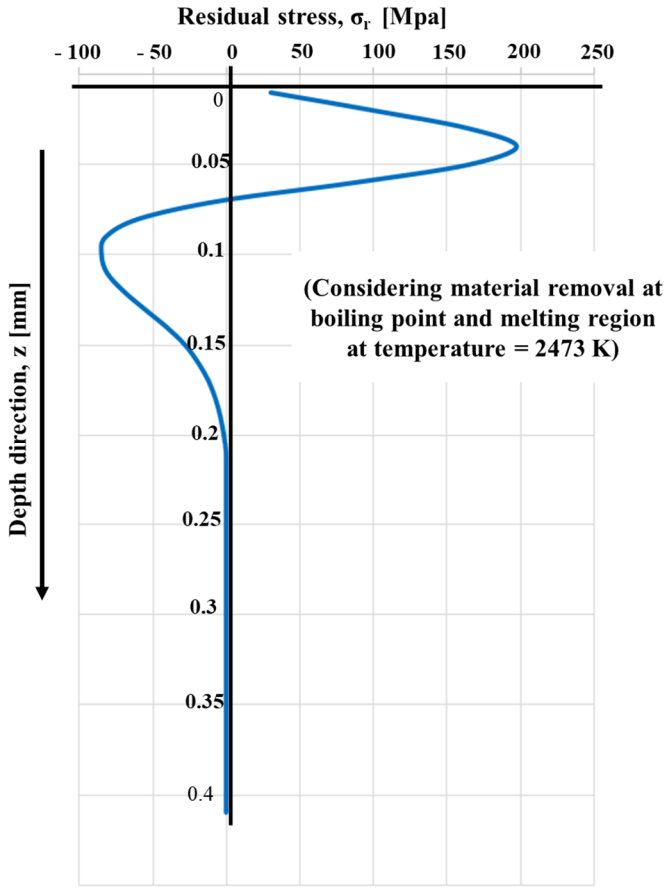

FIGURE 11. Residual stress, σ_r (z) due to single pulse discharge

Modelling of Micro Fin

Actually, and through experience practice, three-dimensional and time-dependent simulation by imposing the thermal stress due to sequential discharges is very complicated and longer time-consuming. For simplification and convenience, it was assumed that the residual stress is two-dimensional, and the stress result considering material removal at boiling point and melting region at temperature = 2473 K as illustrated by Fig. 11 was applied to the beam uniformly along the axis as illustrated in Fig.12. The dimension of the model was based on the machined micro fin as illustrated in Fig. 13 a. Young's Modulus and Poisson ratio was set equal to 2.0×10^{11} Pa and 0.275, respectively.

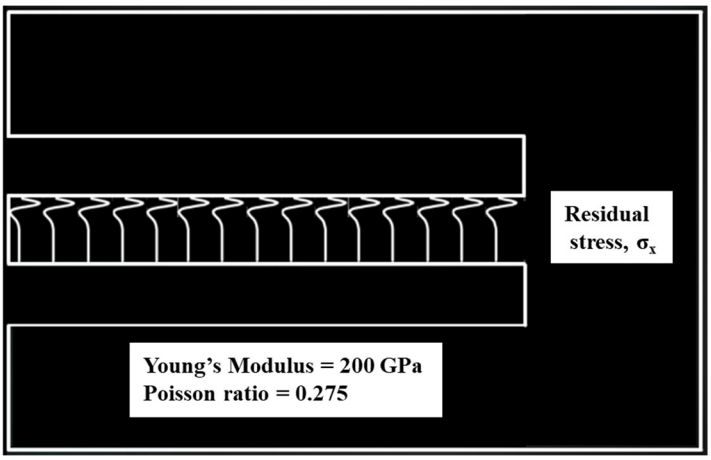

FIGURE 12. Applied residual stress, σ_x within the model

RESULTS AND DISCUSSIONS

The calculation of the process of deformation as suggested by Zahiruddin and Kunieda [11] in their study, was carried out in the current work. The deformation results are depicted in Fig. 13. As seen in Fig. 13 b., after the first deformation process, the residual stress distribution will be released to some extent. Then, the next sequential discharges will be ignited over the fin surface continuously. Consequently, by using the micro fin deformed shape and the residual stress distribution within the micro fin, another same residual stress caused by discharge should be applied only in the area near the micro fin top surface. In other words, the residual stress near the top surface only is replaced by the residual stress distribution due to discharge which is the same as the first deformation process. Distribution of residual stress in another area should be left the same as that was generated after the first deformation process. Subsequently, as a result the newly applied residual stress, the second deformation process is calculated.

As a consequence, the micro fin will deform once more, consequently the distribution of residual stress will be renewed. In the second deformation process, the increment of λ will be smaller than that in the first deformation process. Because the main reason is another deformation in the second process will increase the tensile stress on the bottom surface of the micro fin further. After that, the third deformation process is calculated by using the newly deformed shape for the micro fin and residual stress distribution within the micro fin as the initial conditions. The distribution of residual stress near the top surface of the micro fin is replaced by the same distribution that was distributed on the original surface during the first process since the new discharge craters cover the top surface of the micro fin for the third time. The micro fin deforms even further as a result. Nevertheless, the increase in the second deformation process would be smaller. In the same way, the deformation process is repeated until the micro fin deformed shape in the steady state does not change. Consequently, the calculation of deformation process must be repeated until the change in the micro fin shape does not occur. In theory, the distribution of residual stress before bending should be equal to that after bending in the steady-state. In other words, the original residual stress distribution due to discharge on the top surface should balance with the distribution of residual stress in the bottom side of the micro fin. However, it is difficult to use the deformed shape of the micro fin as an initial condition for the next sequence of discharges. Therefore, for simplification, the deformation of the straight micro fin with the stress fields caused by the previous sequential discharges is obtained. This means, the value of λ based on this calculation method will indicate the increment of micro fin deflection in the ideal calculation which was explained above. Consequently, the summation of all λs which are calculated using straight micro fin as an initial condition should be equal to the final λ obtained from the ideal calculation. Fig. 13 c. and d. show the results of calculation models that used straight micro fin as an initial condition imposed with the stress field due to the two and three sequential discharges, respectively. As illustrated in the figures, λ was equal to 0.197 and 0.06 mm, respectively.

In this example, λ decreased and in theory, it will equal to zero at steady state, which means the residual stress distribution due to discharges on the top surface of fin is equalised with the distribution of residual stress in the bottom side of fin. In Fig. 13 b., c. and d., the overall values of λ was almost equal to the measured deflection value. This interprets that, the deformation of micro fin in this example was the result of stress fields generated by sequential discharges.

As illustrated in Fig. 13 a. and b., although λ was different, experimental and simulation results show that similar bending which is not uniform along the axis of the micro fin. The micro fin looks straight near the root and bending is larger near the tip. Unlike results obtained by Zahiruddin and Kunieda [11] in case of micro EDM, that indicates that the micro fin looks straight near the tip and bending is larger near the root .Theoretically, the distribution of residual stress in the direction of fin thickness should be linear and symmetrical about the boundary between compressive and tensile area in order to form a uniform curvature. However, as seen in Fig. 11, the distribution of residual stress in the thickness direction, $\sigma_r(z)$ was not linear, and this might lead to non-uniform bending.

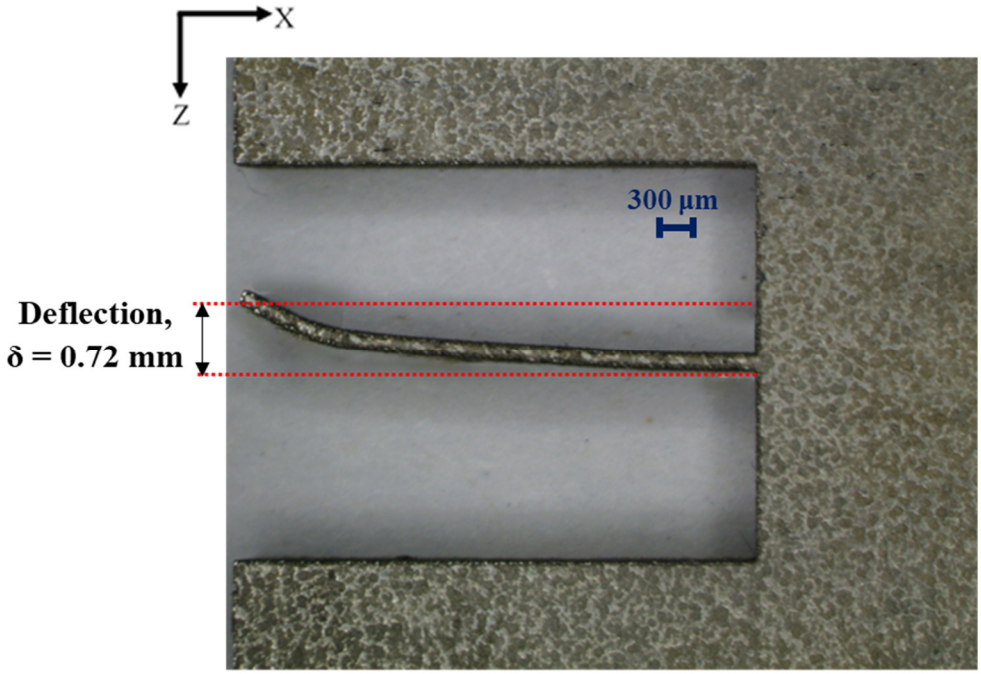

(a)

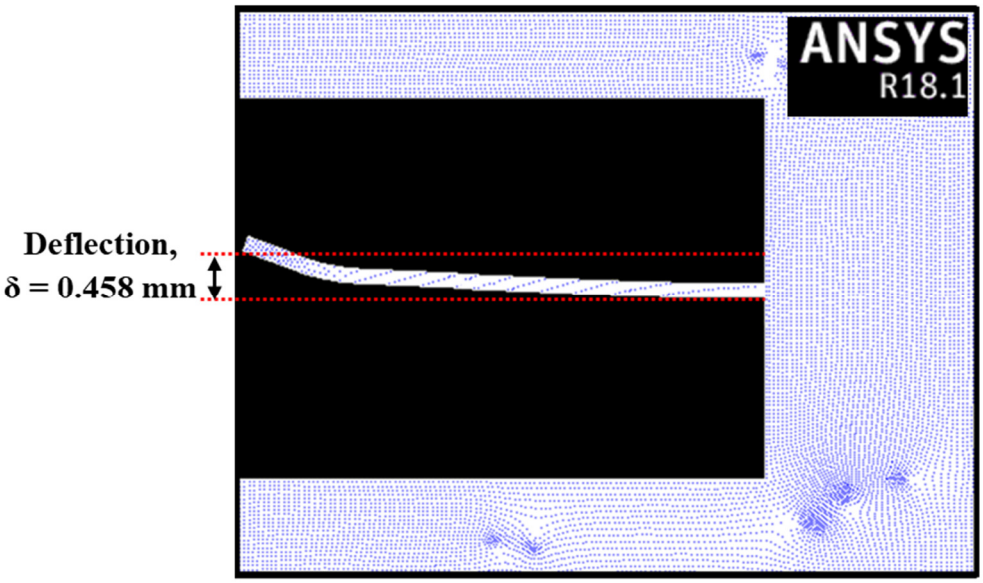

(b)

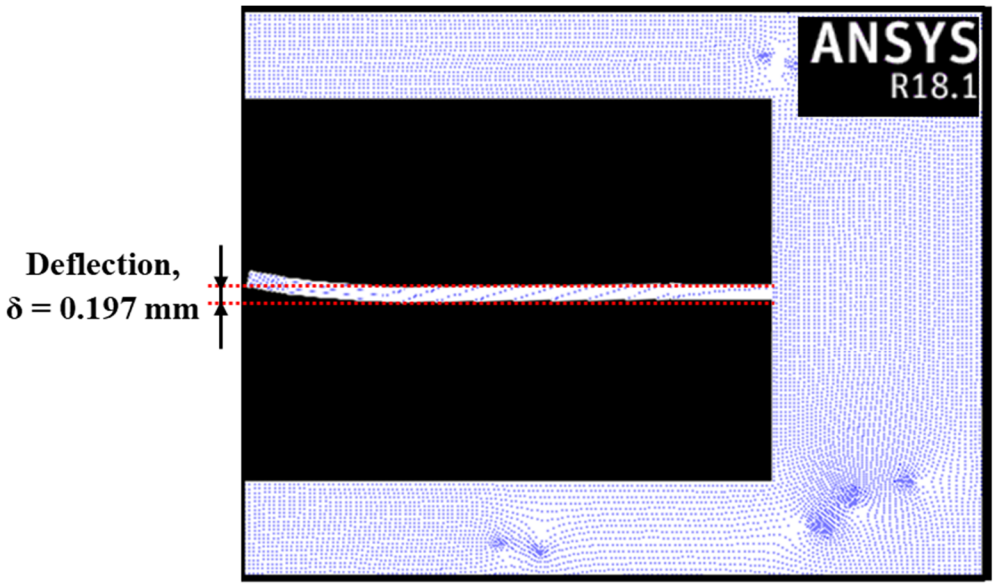

(c)

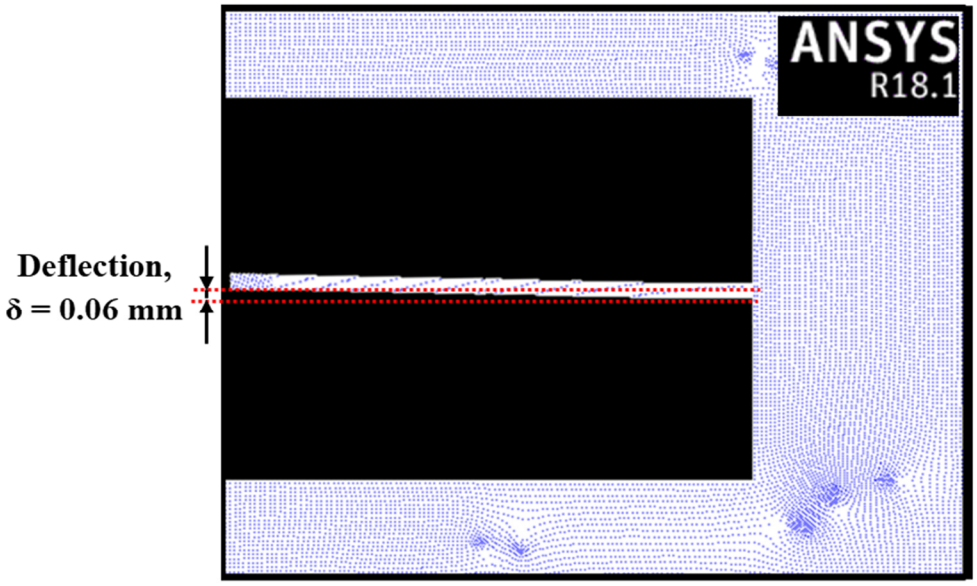

(d)

FIGURE 13. Deformation of fabricated and simulated micro fin (a) Machined micro fin (b) Residual stress due to single discharge uniformly imposed along the fin length (c) Nearly straight micro fin imposed with stress field due to second sequential discharges (d) Straight micro fin imposed with stress field due to third sequential discharges

CONCLUSIONS

In this paper, a new method of applying residual stress within micro fin model was proposed. Besides that, the deformation of micro fin due to WEDM has been studied and this work can be concluded as follows:

- Under WEDM crater, the distribution of residual stress imposed was non-linearly distributed in the thickness direction.
- In order to simulate micro fin deformation, a two-dimensional residual stress was assumed, and the radial residual stress generated by a single discharge was applied to the fin uniformly along the axis. The dimensions of the model, were based on the actual size of micro fin machined by WEDM.
- As a result, a non-uniform bending of the micro fin along its length due to WEDM can be clearly seen. Structural analysis was conducted in order to show the residual stress which was non-linearly distributed in the direction of fin thickness is the main reason that causes the non-uniform bending of the micro fin along its length.
- The curvature of simulated micro fin was similar to that of machined micro fin. As a consequence, this result indicates that the residual stress distribution generated by multi-discharges in the depth direction is similar to the residual stress distribution generated by a single discharge.
- Field of thermal stress due to series of sequential discharges covering the micro fin surface was applied inside the straight micro fin model, and the deflection indicates the increment of micro fin deflection. The deflection decreased with the number of series of sequential discharges and approached to zero. The total value of deflections after three sequential discharges based on the simplified model was approximately equal to the measuring result. This indicates that the deformation of micro fin may result from interaction of stress field due to approximately three sequential discharges.
- Above the thickness of 0.25 mm, the fins show no deflection because of a sufficient ratio of thickness to stress penetration, which avoids deformation occurred. Otherwise, the beams of 0.2 mm and 0.1 mm show warping to the right. In other word, deflection towards the last machining path. The larger curvature was observed at the tip of the micro fin.
- To understand the behaviour and deformation of micro fin, the curvature of a machined micro fin should be compared to the curvature of a simulated micro fin, as well as the distribution of residual stress generated by multiple discharges in the depth direction and distribution of residual stress generated by a single discharge.
- As temperature rises due to an increase in discharge current during the process, residual stresses generated by the machining allow contour elements to deflect in form.

ACKNOWLEDGMENTS

The authors gratefully would like to acknowledge the support from the Fundamental Research Grant Scheme (FRGS) under a grant number of FRGS/6/2016/UniMAP/PPPI/9003-00573 from the Ministry of Education Malaysia.

REFERENCES

1. T. Kawakami and M. Kunieda, Annals of the CIRP 54, 167-170 (2005).
2. G. Spur, E. Uhlmann, U. Doll and N. Daus, IJEM 4, 41-46 (1999).
3. Y. Yang and Y. Mukoyama, IJEM 1, 27–33 (1996).
4. S. Das, M. Lots and F. Klocke, J. of Mater. Process Tech. 142, 434-451(2003).
5. X. Cheng, X. Yang, G. Zheng, Y. Huang and L. Li, J. Mech. Sci. Tech. 28, 2329–2335 (2014).
6. JA. Sanchez, S. Plaza, N. Ortega, M. Marcos and J. Albizuri, Int. J. Adv. Manuf. Tech. 48, 1420–1428 (2008).
7. JA. Sanchez, JL. Rodil, A. Herrero, LL. De Lacalle and A. Lamikiz, J. Mater. Process. Tech. 182, 574–579 (2007).
8. T. Masuzawa, M. Fujino, K. Kobayashi, T. Suzuki, & N. Kinoshita, CIRP Annals 34, 431-434 (1985).
9. A. Warregh and M. Zahiruddin, International Journal of Engineering & Technology 7, 448-455 (2018).
10. A. Kojima, M. Nastu and M. Kunieda, Annals of the CIRP 57, 203-207 (2008).
11. M. Zahiruddin and M. Kunieda, Annals of the CIRP 42, 569-574 (2016).
12. A. Warregh and M. Zahiruddin, “Experimental investigation of workpiece deformation due to WEDM” (International Conference on Advanced Manufacturing and Industry Applications, 2018), pp. 1- 12.
13. A. Warregh and M. Zahiruddin,“Modeling, simulation and investigation of temperature profile during WEDM discharging for stainless steel grade AISI316 material” (AIP Conference Proceedings, 2018), pp. 020102